EVOLUTION OF THE FLARE CAL/VAL SYSTEM TO A MOBILE PLATFORM

Brandon J. Russell [(1)], Chris Durell [(1)], Jeff Holt [(1)]

[(1)] Labsphere, Inc., 231 Shaker St., North Sutton, NH USA 03026, +1 603 927 1104, brussell@labsphere.com

ABSTRACT

FLARE is a new calibration/validation methodology for radiometric and spatial assessment of aerial and satellite imagers. An independent, fully autonomous network of nodes accessed through a cloud interface, FLARE has a unique scalable absolute calibration capability for GSDs ranging from < 5 cm to 30 m. FLARE's SI-traceable methodology augments traditional reflectance and radiometric calibration techniques. FLARE is a true point source and therefore offers powerful, omnidirectional spatial validation of Point Response Function (PRF), band-to-band registration, NIIRS ratings, Modulation Transfer Function (MTF), and other fundamental image quality metrics. The technology is validated with industry, scientific, and government partners. The original FLARE nodes are large, > 3.5m in diameter. The technology has matured over the last 2.5 years of network activity, and newly developed systems offer similar capability at reduced size and cost. These semi-mobile nodes can be commissioned quickly at any suitable site. The first will be deployed at South Dakota State University and USGS EROS for evaluation and experimentation. Within the next year, both types of FLARE node will be installed in partnership with the NOAA ESRL Mauna Loa Observatory as a pristine, low uncertainty calibration site at > 3,400 m altitude.

1 INTRODUCTION

Achieving low uncertainty, SI-traceable vicarious calibration of Earth Observation (EO) sensor platforms is critical to scientific, commercial, and government remote sensing programs. This is especially relevant to achieving data harmonization and sensor fusion products across diverse missions and temporal, spatial, and spectral scales. New scalable technologies, methods, and approaches are required to handle ever increasing volumes of remotely sensed data and ensure product quality.

For spaceborne instrumentation, extensive pre-flight radiometric and spatial calibration and characterization is standard practice for well-funded, long duration scientific and government missions. This approach may not be feasible for smaller commercial missions with more limited resources and rapid production, launch, and revisit schedules. Continuous vicarious calibration and inter-comparison efforts on orbit [1]–[5] are critical to maintaining performance and sensor interoperability for any EO program.

Typical radiometric characterization is based on viewing a traceable extended source that uniformly illuminates many, if not all, detectors on the focal plane. Pre-flight, diffuse targets or integrating spheres are used. On-orbit, radiometric calibration includes on-board solar diffusers and light sources, or the viewing of extended targets such as the moon, or large, well characterized sites on Earth such as deserts or salt flats [6], [7]. Illuminating a large number of detectors establishes a mean response to the calibration radiance. Extensive efforts for Sentinel 2, Landsat 8, and other sensors demonstrate the success of this methodology for remote sensing of large areas and targets [2], [8] . However, this

averaging approach is technically valid only for extended uniform scenes for which the response is unaffected by the sensor's image quality performance [9].

Beyond radiometric fidelity, a key component of image quality is spatial and geometric performance. Metrics include band to band registration and absolute geolocation, as well as complex transfer functions that govern the overall resolution, blur, or target separability, and Ground Sample Distance (GSD). System resolution is a complex parameter encompassing the performance of the entire optical system [10], [11]. High contrast targets like coastlines, bridges, airports, or purpose-built contrast arrays are utilized to assess the Edge/Point/Line Spread Functions (ESF/PSF/LSFs), Modulation Transfer Function (MTF), spectral band co-registration, Rayleigh criteria, and blur metrics [12]–[14].

The SPecular Array Radiometric Calibration (SPARC) method employs convex mirrors to relay an image of the solar disk to create arrays of calibration targets for deriving absolute calibration coefficients in the solar reflective spectrum [9], [15]. The mirrors create a sub-pixel point source, useful for both spatial and radiometric characterization of the sensor, especially when viewing small targets [16]. By varying mirror curvature, diameter, and number, it is possible to produce a large dynamic range of at-sensor radiance suitable to a variety of instrument classes. With appropriate solar radiometric measurements, the SPARC target can then be used as an absolute reference for at-aperture spectral radiance [16], [17] or surface reflectance [18]. The use of mirrors allows for simplification of the optical corrections necessary for derivation of radiometric or surface parameters, in comparison to diffuse reflectance targets [16]. In the spatial domain, an over-sampled point source can be used to assess system resolution metrics such as MTF, Point Response Function, band registration, blur, defocusing, cross and along track smear, Rayleigh and Sparrow Criteria, or image processing artifacts. As sub-pixel impulse targets, the mirrors are omni-directional and do not need to be oriented relative to the sensor's orbital path and are consistent when viewed from any direction, including off-nadir.

Combining SPARC mirrors with automated targeting, instrumentation, and communications equipment is the basis for the new Field Line-of-sight Automated Radiance Exposure (FLARE) Network [17]. FLARE is an on-demand, accessible system for International System (SI) traceable, absolute radiometric and geometric calibration and validation. With improved understanding of radiometric performance compared to other in-flight vicarious techniques, FLARE can reduce uncertainties in target reflectance, atmospheric effects, and temporal variability. The network provides a unique tool to enhance current vicarious calibration and validation (cal/val) programs and will augment existing techniques like RadCalNet [6], [19], Pseudo Invariant Calibration Sites (PICS) [7], [20], or targeted overpass efforts. In particular, point sources serve as a reference and diagnostic tool for small target radiometry, revealing performance characteristics at spatial scales below that of large geographic features where blur and averaging can conceal non-uniform response. Importantly and uniquely, the point target approach of SPARC and FLARE can be scaled across a huge range of spatial sampling resolutions from centimeters (e.g. drones) to decameters (e.g. Landsat 8 OLI) and even to larger footprints in the hundreds of meters or greater. The performance of FLARE and the SPARC method has been validated with multiple commercial constellations and agency sensors [9], [15], [17], [18], [21], [22].

Currently, two FLARE nodes are operational with planned expansion of the network across geographic, climatic, and atmospheric gradients. The first two installations in Arlington, SD USA and Brock, TX, USA are relatively large, requiring a semi-permanent installation of mirrors, power, communications, and radiometric instrumentation. Referred to as "*Beacon*s," these systems provide a fixed point capable of generating a wide dynamic range of radiance, from background to saturation,

suitable for UAV, airborne, or satellite sensors with Ground Sample Distances between ~5 cm and ~ 30 m (Fig. 1). A third node is in production which represents a lower cost, smaller, lighter, and easier to install instrument with mission-specific radiometric capability. Dubbed "*Lantern*," this node type was designed to provide a functional but non-contiguous range of radiance levels for a specific GSD. *Lantern*s can be deployed either as a fixed installation or transported to a selected location for targeted cal/val campaigns. In fact, the first *Lantern* will be deployed alongside the Arlington, SD *Beacon* as part of an upcoming experiment to validate Sentinel 2 surface reflectance products.

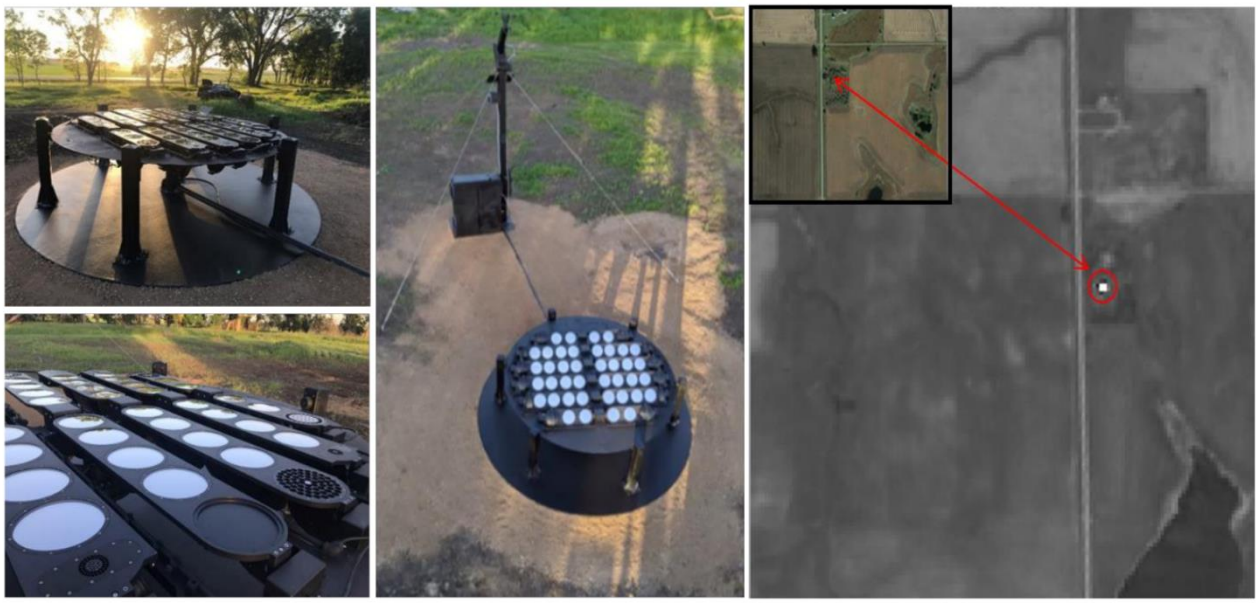

Figure 1. *Beacon* node installed at agricultural test site, Arlington, SD. The activated array is clearly visible in Sentinel 2B imagery (right). Inset image courtesy Google Earth. Figure reproduced from [17].

2 FLARE SYSTEM DESIGN

The *Beacon* nodes are highly capable fiducial stations that can serve a wide range of sensor platforms and mission types, and as such are the foundation points of the FLARE Network. As a result of these requirements, they are complex, expensive, and necessarily constrained to a fixed location. The *Lantern* nodes (Fig. 2) were developed to enable the construction of a much greater number of automated systems, either at distributed sites, placed alongside targets of interest for specific operations, or grouped together in order to provide multiple points within the same scene.

A full-function FLARE Node consists of an addressable mirror array, solar spectroradiometer, and power/communications/control equipment [17]. While the exact configurations of these components will vary between *Beacon* and *Lantern* classes and individual sites, the basic functions are common to all FLARE nodes. The foundational operation mode of the system is an automated "LOOK." This event is user defined and scheduled online, and the operation of the system is automated. The system opens the appropriate mirrors for the desired signal level and positions the mirrors to relay the solar signal to the targeted craft; continuously tracking through a defined trajectory across the sky. During a LOOK, the station also performs the necessary radiometric measurements to model the upwelling and downwelling atmospheric optical transmission necessary to derive absolute calibration values. Finally, the mirrors are covered in a weather and dust proof

housing and data is transmitted. Access to all networked nodes is through a web-based portal where registered users can schedule events, download data, and upload imagery for processing. Users can task the network and upload imagery for analysis either with a web-based portal, or an Application Programming Interface (API) created for integration of the network's capabilities into existing data-handling architecture.

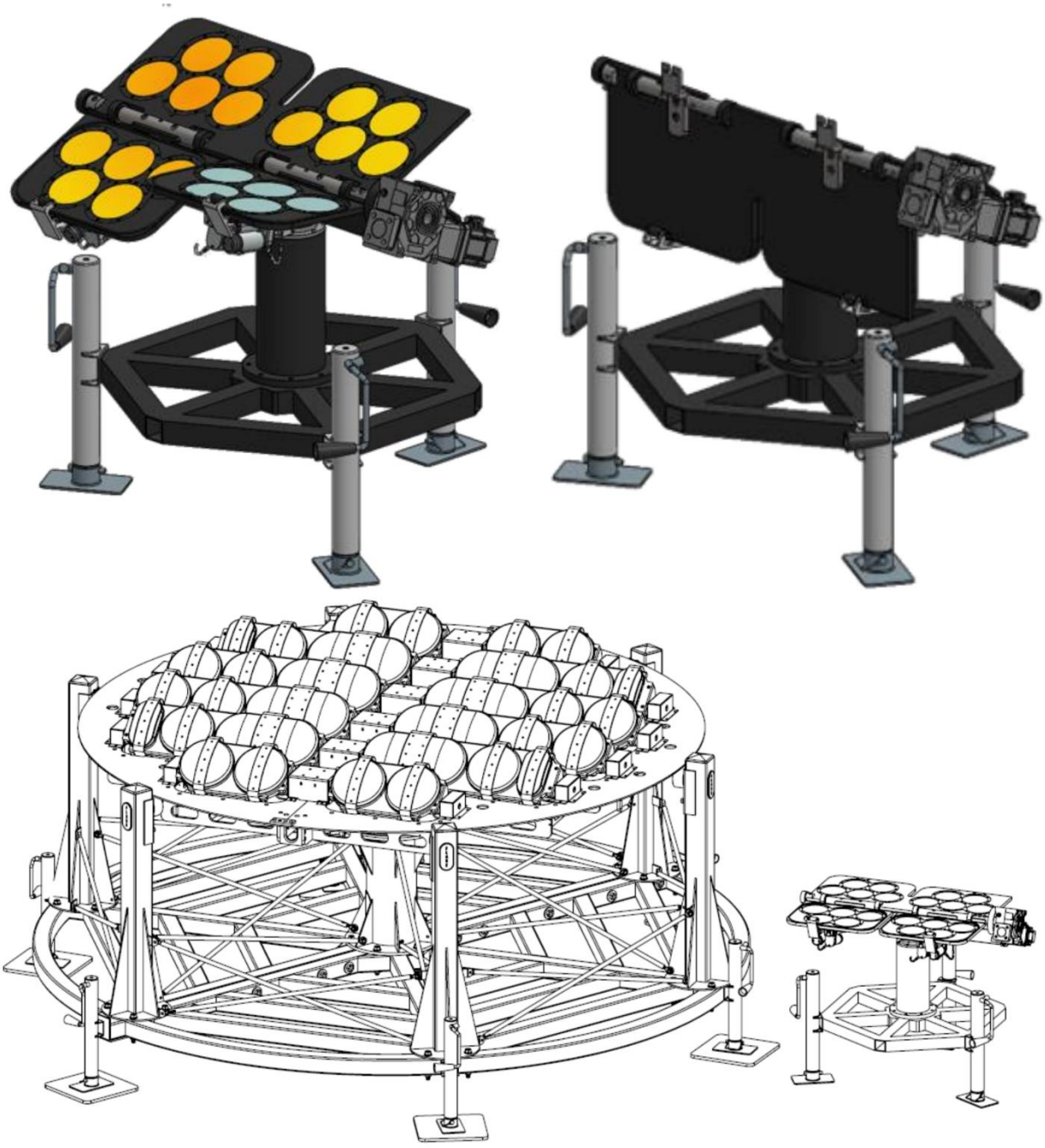

Figure 2. Design models of the upcoming *Lantern* nodes (top). Dynamic range is controlled by opening and pointing individual plates (left), and plates can be sealed to protect mirrors from dirt and debris (right). *Lantern* nodes will be ~ 35% the size and weight of *Beacons (bottom).*

2.1 Control Equipment

Associated with the system is a suite of control, communications, and power handling equipment. These are housed in a weather-proof electronics cabinet. All communications are handled through a cellular modem and power is supplied either with direct wiring or solar panels, depending on the specific installation. A set of cameras attached to the mirror turret or radiometer are used for data quality and diagnostic checks, which can be useful in explaining any data anomalies [23], atmospheric conditions, or identifying a need for servicing.

2.2 Mirror Array Turrets

A FLARE mirror turret consists of azimuth and elevation tracking motors, with either individual mirror bays (*Beacon*) or mirror plates (*Lantern*). Both types are designed to be modular and can accommodate multiple mirror types, allowing flexibility in signal characteristics. In the *Beacon* nodes, each mirror bay has a cover used to control dynamic range and to protect the mirror surfaces from degradation due to environmental exposure. For *Lantern* nodes, multiple mirrors are placed on 4 individual plates and dynamic range is controlled by pointing the plates either on or off-axis. The plates seal against each other and stow vertically to prevent intrusion of water, dirt, or insects.

At any point during the real-time execution of a FLARE overpass, the angular position of the mirrors is known. Given a specific mirror configuration and execution angles, the effective signal center may be calculated and located to an absolute position on the Earth. For permanent or long-term installations, a high accuracy GPS survey of the site is conducted in order to serve as a Ground Control Point (GCP) or geolocation verification point.

As determined by the radiometry of specular targets [17], the number, diameter and radius of curvature of the mirror population creates a trade space for tuning a particular node to different classes of sensor, as well as determining dynamic range. The *Beacon*s are optimized for validation of mid-resolution Earth Observation sensors, specifically Sentinel 2 A/B MSI, PRISMA, and Landsat 8 OLI which have GSDs between 10 and 60 m. However, these have mirror subsets designed for higher resolution down to sub-meter GSDs. *Lantern* turrets are equipped to provide a limited number of signal strengths across the dynamic range of ~ 5 – 20 m GSD class sensors, for example the Sentinel-2 VNIR bands (Fig. 3). Mirror plates can be manually replaced for larger or smaller GSDs. *Beacon* stations can produce radiance levels (Fig. 3, dotted lines) over a range equivalent to dark vegetative targets to deep convective clouds, with approximately 28 levels of adjustability. While not capable of producing as strong a signal, the *Lantern* semi-mobile nodes have a maximum radiance well above most terrestrial targets, with 4 levels of range (Fig. 3, dashed lines) from the Sentinel 2 reference radiance at the lower limit to radiance equivalent to a 100% reflective Lambertian target.

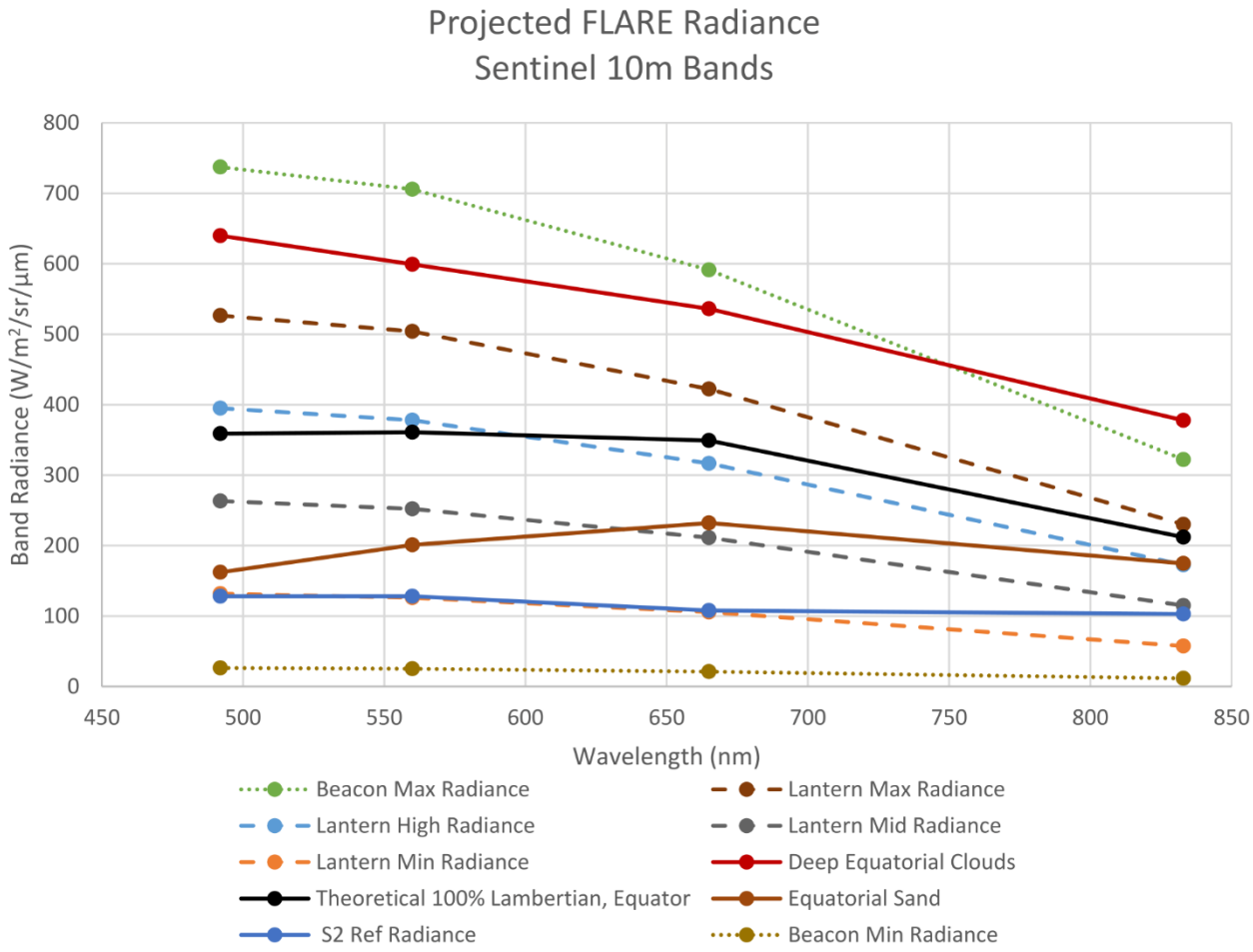

Figure 3. As illustrated for the Sentinel 2 MSI 10 m VISNIR bands, all FLARE nodes have been designed to produce SI-traceable radiance signals across the dynamic range of targets encountered by Earth Observation missions.

2.3 Radiometric Instrumentation

Any FLARE node can be configured to include a solar radiometer, either as an independent articulated tower for *Beacon*s or as an integrated unit into a *Lantern* mirror plate. The *Beacon* radiometer consists of a tracking head, fore optics, VISNIR spectrometer, banded SWIR detector, and a halogen-based calibration source. The spectrometer is a modified CDS-2600 (Labsphere) which provides radiometric data between 350 – 1075 nm at 2.4 nm resolution, with data resampled to 1 nm intervals and corrected for stray light. The SWIR detector has 8 bands between 800 and 2500 nm. The optical benches are thermo-electrically cooled and contained in a temperature-controlled housing. When inactive, the radiometer head is sealed against a weather-resistant compartment to maintain cleanliness of the optics. The *Lantern* radiometer utilizes a similar optical bench, but with modified fore optics integrated into one of the mirror plates. Pointing capability is achieved using the turret itself rather than an articulated tower. In both systems, a modified version of the Langley regression method [24] is employed for calibration of instrument response, traceable to the TSIS-1 solar radiometer [25] on the International Space Station. An on-board NIST-traceable QTH source offers an alternative calibration methodology for the radiometer.

3 EXPANSION AND DEVELOPMENT OF THE FLARE NETWORK

The addition of *Lantern* nodes to the FLARE Network will enable new capabilities, as well as facilitate expansion of calibration events to new geographic and climatic regions globally. The first *Lantern* node will be deployed in proximity to the Arlington, SD *Beacon* site. Multiple SPARC targets embedded in the same scene, under identical atmospheric conditions, at different radiance levels allows for a response regression across the sensor's dynamic range (Fig. 4).

During a recent multi-agency experiment, Sentinel 2A Top of Atmosphere imagery was corrected to surface reflectance using FLARE. The multispectral reflectance of a vegetative target, specifically an alfalfa field, as reported in the calibrated imagery agreed with in-situ measurements to within the uncertainty of the measurement. This Mirror-based Empirical Line Method (MELM) approach is directly applicable to validation of surface reflectance products [18], particularly for dark targets like agricultural fields or water bodies. Secondly, a robust characterization of a sensor's PRF or MTF requires multiple point source images to account for the aliasing effect induced by pixel phasing. The more point sources available in-scene, the more rapidly such a dataset can be produced. Tests quantifying metrics of sensor resolution, NIIRS ratings, and target separability have shown the utility of mirror point source targets [22], [26], [27]. It is important to note that as point sources are omni-directional, cross and along-track metrics can be generated with the same target.

As part of the evolution of the FLARE Network, *Lantern* nodes are in production that will be optimized for a specific satellite or constellation and maintained at the operator's facility. These nodes will remain connected to the network and accessible to all users through the API or web portal. Operator's use of these nodes for dedicated purposes, as well as usage within the network, will enable proliferation and partnerships that allow for rapid expansion and adoption of FLARE across commercial and agency users. Private use and public access will facilitate both rapid and on-demand characterization of a single sensor as well as community capability for data harmonization and interoperability across platforms.

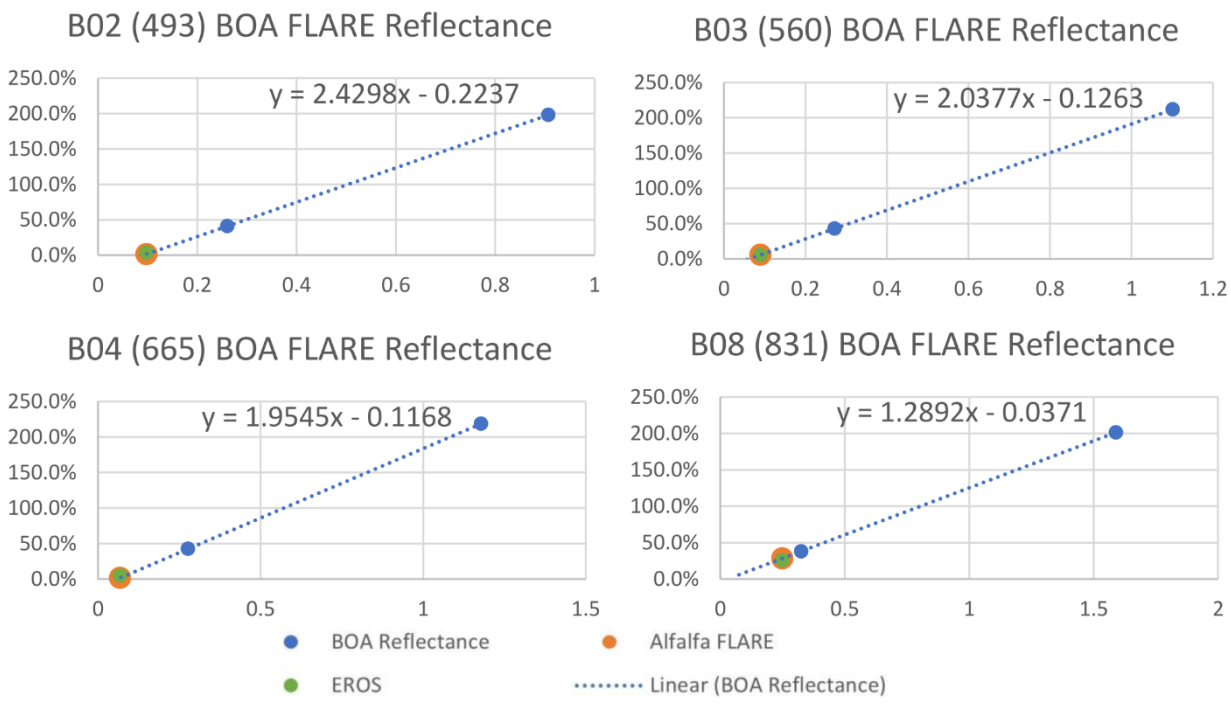

Figure 4. With high and low radiance FLARE targets in scene, it is possible to perform a linear regression of sensor response in either radiance or surface reflectance space. By performing a regression using the mirror targets, the Bottom of Atmosphere reflectance (S2B) of an alfalfa field, had good agreement with ground-truth measurements made by USGS EROS.

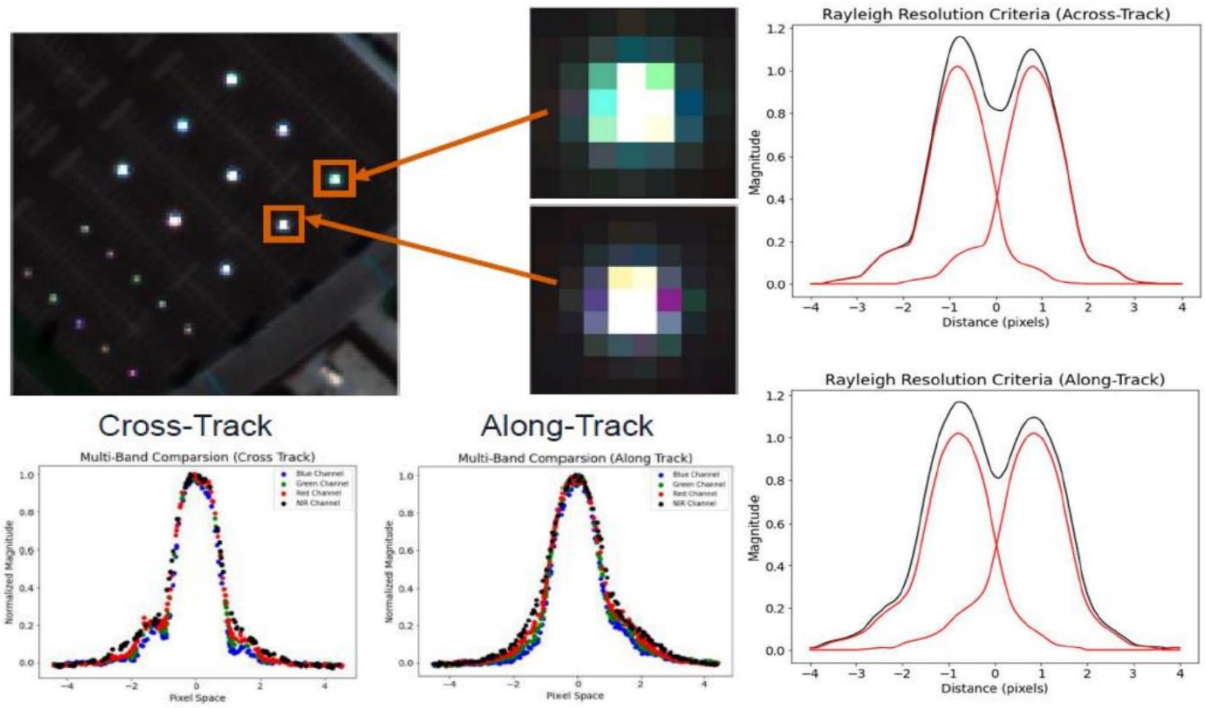

Figure 5. By oversampling a system's Point Response Function with multiple mirror sources, image quality metrics can be produced in any spatial direction.

3.1 FLARE Node - Mauna Loa Observatory

While the FLARE Network is operated as a service, the primary goal is to advance and expand vicarious calibration and validation across the Earth Observation and remote sensing communities. To that end, funded engagement with government and academic institutions using SPARC and FLARE are ongoing. The next major installation of the FLARE Network will be at the NOAA Mauna Loa Atmospheric Baseline Observatory, scheduled to be commissioned in the second half of 2022. Through a cooperative public-private project with the Earth System Research Laboratories, a *Beacon* and *Lantern* node will be placed on the NOAA parcel at 3,400 m above sea level.

The FLARE-MLO node is intended to serve as the Network's premier, low uncertainty calibration location. Situated in an extremely stable atmosphere above the inversion layer, it is expected to achieve radiometric uncertainty < 1.5%. The lava rock at the observatory is an ideal background for SPARC calibration – diffuse, spatially uniform, and low reflectance (~5%) over the 350 – 2500 nm range [28]–[30]. Experiments conducted with manually deployed SPARC targets against Landsat 8 and 9 have demonstrated an excellent contrast and high signal to noise across all OLI bands (Fig. 6).

3.2 Benefits to Mauna Loa Observatory and Other Partners

The FLARE MLO station directly serves NOAA's mission by providing a high-quality calibration site for current and future environmental monitoring missions. Data from the system will be made available directly to NOAA, NASA, NIST, and other researchers to enhance existing solar and atmospheric monitoring activities at MLO. Beyond improved calibration for EO missions, there are several projects at MLO which FLARE can directly benefit. For example, NASA's AErosol RObotic NETwork (AERONET) uses the site as a primary calibration facility for its VNIR multispectral CIMEL sun photometers [24], [31]. Data from the FLARE hyperspectral VNIR and multi-spectral SWIR solar radiometer will be available for algorithm development and validation. The Mauna Loa Observatory Lunar Spectral Irradiance (MLO-LUSI) project, run by NIST, is working to improve measurements of the Moon to enable its use as an absolute reference standard for the dozens of satellites that study and monitor the Earth's weather and climate. The FLARE radiometer will be made available to NIST for lunar observations – the radiometer's SWIR capability has the potential to expand the MLO-LUSI spectral range.

As part of the partnership with MLO, all FLARE hardware at the site is designed for minimal impact, visually, environmentally, culturally, or otherwise. All turret surfaces are black painted or made from optically black materials to minimize the impact of the hardware on the radiometric signal received by a sensor as part of standard system design, and this concept will be extended to any other peripheral components that would be visible from the road or base of Mauna Loa. All equipment installed at the location will have minimal physical footprint and terrain impact – no major flattening or clearing operations on the lava rock are expected as both *Beacon* and *Lantern* systems are self-leveling and stabilized. Earth anchors for protection against wind will be included and all equipment secured. Ultimately, all components of the systems can either be fully removed or deactivated with minimal physical traces upon decommissioning.

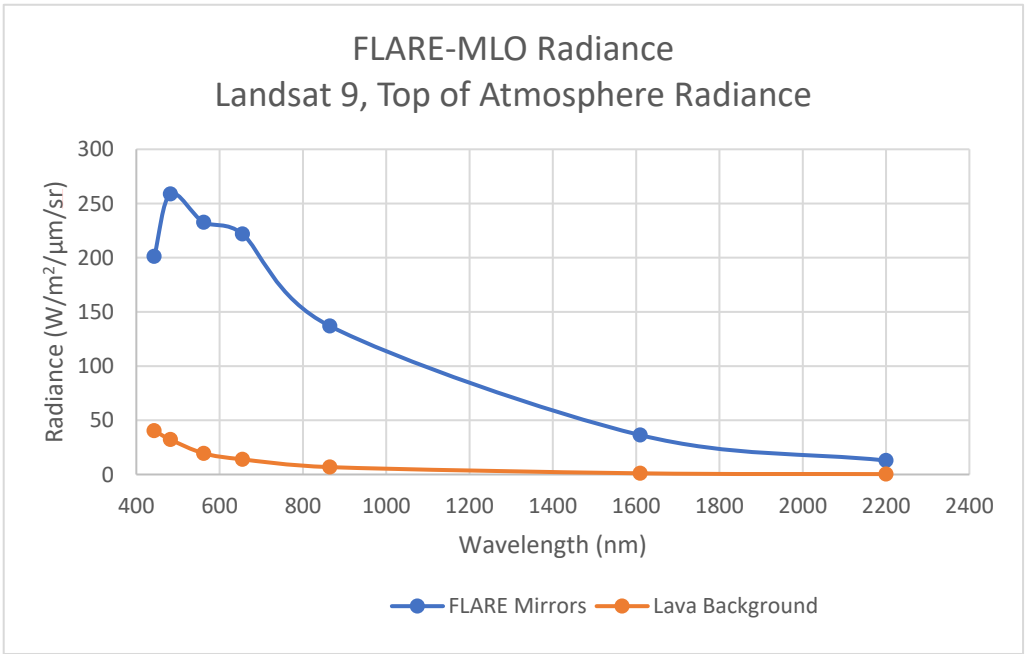

Figure 6. Top: Demonstrations at the Mauna Loa Observatory (inset, top left) with mirror arrays (inset, bottom left), as imaged by Landsat 9 OLI (circled). Bottom: The FLARE-MLO node will achieve high signal-to-background against the dark lava rock, facilitating low uncertainty radiometric calibration across the ~350 to 2500 nm range. Color imagery courtesy Google Earth.

4 CONCLUSIONS AND FUTURE WORK

The FLARE Network represents a new tool for calibration and validation of Earth Observation assets in the VNIR-SWIR spectrum. The use of convex mirrors makes it uniquely capable of scaling across a wide range of EO spatial scales, from 5 cm to 30 m, with even larger pixel sizes possible. Newly developed smaller, more portable versions of the technology will allow rapid expansion of the network, unique calibration locations, new characterization techniques, as well as tailoring stations for validation of individual satellites or constellations. The upcoming installation of a 2-point station on Mauna Loa will create a low uncertainty, high stability calibration site, broadly accessible and intended to facilitate data interoperability, quality, and traceability across academic, commercial, and government remote sensing communities.

REFERENCES

[1] B. Markham *et al.*, "Landsat-8 Operational Land Imager Radiometric Calibration and Stability," p. 34, 2014.

[2] J. Czapla-Myers *et al.*, "The Ground-Based Absolute Radiometric Calibration of Landsat 8 OLI," p. 27, 2015.

[3] J. Gorroño *et al.*, "Providing uncertainty estimates of the Sentinel-2 top-of-atmosphere measurements for radiometric validation activities," *Eur. J. Remote Sens.*, vol. 51, no. 1, pp. 650–666, Jan. 2018, doi: 10.1080/22797254.2018.1471739.

[4] R. Morfitt *et al.*, "Landsat-8 Operational Land Imager (OLI) Radiometric Performance On-Orbit," *Remote Sens.*, vol. 7, no. 2, pp. 2208–2237, Feb. 2015, doi: 10.3390/rs70202208.

[5] A. Loew *et al.*, "Validation practices for satellite-based Earth observation data across communities: EO VALIDATION," *Rev. Geophys.*, vol. 55, no. 3, pp. 779–817, Sep. 2017, doi: 10.1002/2017RG000562.

[6] M. Bouvet *et al.*, "RadCalNet: A Radiometric Calibration Network for Earth Observing Imagers Operating in the Visible to Shortwave Infrared Spectral Range," p. 25, 2019.

[7] M. Shrestha, Md. N. Hasan, L. Leigh, and D. Helder, "Extended Pseudo Invariant Calibration Sites (EPICS) for the Cross-Calibration of Optical Satellite Sensors," *Remote Sens.*, vol. 11, no. 14, p. 1676, Jul. 2019, doi: 10.3390/rs11141676.

[8] S. Kabir, L. Leigh, and D. Helder, "Vicarious Methodologies to Assess and Improve the Quality of the Optical Remote Sensing Images: A Critical Review," *Remote Sens.*, vol. 12, no. 24, p. 4029, Dec. 2020, doi: 10.3390/rs12244029.

[9] S. J. Schiller and J. Silny, "The Specular Array Radiometric Calibration (SPARC) method: a new approach for absolute vicarious calibration in the solar reflective spectrum," San Diego, California, United States, Aug. 2010, p. 78130E. doi: 10.1117/12.864071.

[10] R. D. Fiete, *Modeling the imaging chain of digital cameras*. Bellingham, Wash: SPIE Press, 2010.

[11] A. Q. Valenzuela and J. C. G. Reyes, "Basic Spatial Resolution Metrics for Satellite Imagers," *IEEE Sens. J.*, vol. 19, no. 13, pp. 4914–4922, Jul. 2019, doi: 10.1109/JSEN.2019.2902512.

[12] M. Pandžic, D. Mihajlovic, J. Pandžic, and N. Pfeifer, "ASSESSMENT OF THE GEOMETRIC QUALITY OF SENTINEL-2 DATA," *ISPRS - Int. Arch. Photogramm. Remote Sens. Spat. Inf. Sci.*, vol. XLI-B1, pp. 489–494, Jun. 2016, doi: 10.5194/isprsarchives-XLI-B1-489-2016.

[13] F. Languille *et al.*, "Sentinel-2 geometric image quality commissioning: first results," Toulouse, France, Oct. 2015, p. 964306. doi: 10.1117/12.2194339.

[14] B. Wenny, D. Helder, J. Hong, L. Leigh, K. Thome, and D. Reuter, “Pre- and Post-Launch Spatial Quality of the Landsat 8 Thermal Infrared Sensor,” *Remote Sens.*, vol. 7, no. 2, pp. 1962–1980, Feb. 2015, doi: 10.3390/rs70201962.
[15] S. J. Schiller, M. Teter, and J. Silny, “Comprehensive vicarious calibration and characterization of a small satellite constellation using the Specular Array Calibration (SPARC) method,” 2017, p. 12.
[16] S. Schiller and J. Silny, “Using vicarious calibration to evaluate small target radiometry,” presented at the 25th Annual Meeting on Characterization and Radiometric Calibration for Remote Sensing, Logan, Utah, 2016.
[17] B. Russell *et al.*, “Initial results of the FLARE vicarious calibration network,” in *Earth Observing Systems XXV*, Online Only, United States, Sep. 2020, p. 14. doi: 10.1117/12.2566759.
[18] J. D. Ortiz *et al.*, “Intercomparison of Approaches to the Empirical Line Method for Vicarious Hyperspectral Reflectance Calibration,” *Front. Mar. Sci.*, vol. 4, p. 296, Sep. 2017, doi: 10.3389/fmars.2017.00296.
[19] J. Czapla-Myers, M. Bouvet, and B. Wenny, “The Radiometric Calibration Network (RadCalNet): a Global Calibration and Validation Test Site Network,” 2016, doi: 10.13140/RG.2.2.30866.86720.
[20] N. Mishra, D. Helder, A. Angal, J. Choi, and X. Xiong, “Absolute Calibration of Optical Satellite Sensors Using Libya 4 Pseudo Invariant Calibration Site,” *Remote Sens.*, vol. 6, no. 2, pp. 1327–1346, Feb. 2014, doi: 10.3390/rs6021327.
[21] J. Lekki, S. Ruberg, C. Binding, R. Anderson, and A. Vander Woude, “Airborne hyperspectral and satellite imaging of harmful algal blooms in the Great Lakes Region: Successes in sensing algal blooms,” *J. Gt. Lakes Res.*, vol. 45, no. 3, pp. 405–412, Jun. 2019, doi: 10.1016/j.jglr.2019.03.016.
[22] B. Russell *et al.*, “The FLARE Network: Vicarious Cal/Val for Earth Observation Satellites,” in *35th Annual Small Satellite Conference*, 2021, p. 9.
[23] D. Vansteenwegen, K. Ruddick, A. Cattrijsse, Q. Vanhellemont, and M. Beck, “The Pan-and-Tilt Hyperspectral Radiometer System (PANTHYR) for Autonomous Satellite Validation Measurements—Prototype Design and Testing,” *Remote Sens.*, vol. 11, no. 11, p. 1360, Jun. 2019, doi: 10.3390/rs11111360.
[24] B. N. Holben *et al.*, “AERONET—A Federated Instrument Network and Data Archive for Aerosol Characterization,” *Remote Sens. Environ.*, vol. 66, no. 1, Art. no. 1, Oct. 1998, doi: 10.1016/S0034-4257(98)00031-5.
[25] E. Richard *et al.*, “SI-traceable Spectral Irradiance Radiometric Characterization and Absolute Calibration of the TSIS-1 Spectral Irradiance Monitor (SIM),” *Remote Sens.*, vol. 12, no. 11, Art. no. 11, Jun. 2020, doi: 10.3390/rs12111818.
[26] B. Russell, J. Holt, C. Durell, W. Arnold, D. Conran, and S. Schiller, “The Flare: Network: Autonomous, On-Demand Spatial and Radiometric Calibration and Validation for Imaging Spectroscopy,” in *2021 IEEE International Geoscience and Remote Sensing Symposium IGARSS*, Brussels, Belgium, Jul. 2021, pp. 1615–1618. doi: 10.1109/IGARSS47720.2021.9554741.
[27] D. Conran *et al.*, “A New Technique to Define the Spatial Resolution of Imaging Sensors,” in *2021 IEEE International Geoscience and Remote Sensing Symposium IGARSS*, Brussels, Belgium, Jul. 2021, pp. 8158–8161. doi: 10.1109/IGARSS47720.2021.9554436.
[28] L. Li, C. Solana, F. Canters, J. Chan, and M. Kervyn, “Impact of Environmental Factors on the Spectral Characteristics of Lava Surfaces: Field Spectrometry of Basaltic Lava Flows on Tenerife, Canary Islands, Spain,” *Remote Sens.*, vol. 7, no. 12, pp. 16986–17012, Dec. 2015, doi: 10.3390/rs71215864.

[29] S. Amici, A. Piscini, and M. Neri, “Reflectance Spectra Measurements of Mt. Etna: A Comparison with Multispectral/Hyperspectral Satellite,” *Adv. Remote Sens.*, vol. 03, no. 04, pp. 235–245, 2014, doi: 10.4236/ars.2014.34016.
[30] M. Abrams, E. Abbott, and A. Kahle, “Combined Use of Visible, Reflected Infrared, and Thermal Infrared Images for Mapping Hawaiian Lava Flows,” *J. Geophys. Res.*, vol. 96, no. B1, pp. 475–484, Jan. 1991.
[31] C. Toledano *et al.*, “Assessment of Sun photometer Langley calibration at the high-elevation sites Mauna Loa and Izaña,” *Atmospheric Chem. Phys.*, vol. 18, no. 19, Art. no. 19, Oct. 2018, doi: 10.5194/acp-18-14555-2018.